sustainability

MDPI

Article

Simulating the Hydraulic and Volume Change Behavior of Compacted Highly Expansive Soil under Potential Field Stress and Seasonal Climatic Variation

Mohamed Farid Abbas [1,2]

[1] Department of Civil Engineering, College of Engineering in Al-Kharj, Prince Sattam bin Abdulaziz University, Al-Kharj 11942, Saudi Arabia; m.abbas@psau.edu.sa or moh_farid_apas@yahoo.com
[2] Soil Mechanics and Geotechnical Engineering Research Institute, Housing and Building National Research Center (HBRC), Giza P.O. Box 1770, Egypt

Abstract: A sustainable design of some engineering applications, such as earth dam cores, landfill liners, clay barriers, and radioactive waste disposal systems, that utilize compacted expansive soils requires simulation for probable field conditions. This study investigated the hydraulic and volume change (H-VC) behaviors of highly expansive compacted soils in Al-Qatif city under different seasonal climatic variations for a wide range of stress conditions, aiming for more economical and rational design and practices. The extent of the effect of the start cycle condition of the cyclic wetting and drying (W/D) process on the examined properties is examined, as well. Two testing series of the cyclic W/D process, representing the probable seasonal climatic variations, were executed for varied axial stress conditions. The H-VC behaviors of expansive soils are affected by the simulated seasonal variation (i.e., cyclic W/D process), with the first cycle of W/D being the most effective cycle and an elastic state being attained by the third to fourth cycle. Swell fatigue is noted for both testing series, and this is attributed to the initial placement condition. Analysis of results recommends exposure of the compacted expansive soil layers in the field to drying after compaction to reduce their equilibrium wetting potential. As a consequence of the noted shrinkage accumulation, a reduction tendency of saturated hydraulic conductivity (k_{sat}) with repeated W/D cycles is reported for both series under all the stress states applied. Finally, it is recommended for clay barrier projects to be submerged once compacted to obtain barriers with the lowest values of hydraulic conductivity.

Keywords: expansive soils; hydraulic conductivity; volume change potential; cyclic wetting and drying

Citation: Abbas, M.F. Simulating the Hydraulic and Volume Change Behavior of Compacted Highly Expansive Soil under Potential Field Stress and Seasonal Climatic Variation. *Sustainability* **2023**, *15*, 10797. https://doi.org/10.3390/su151410797

Academic Editors: Yutao Pan, Qiujing Pan and Hui Xu

Received: 19 April 2023
Revised: 30 May 2023
Accepted: 25 June 2023
Published: 10 July 2023

1. Introduction

Expansive soil, which is characterized by its tendency to undergo volume change (VC) when exposed to moisture variations, has naturally existed globally over wide areas and may be used as compacted material in different engineering applications. Hence, it may be exposed in the field to a wide range of applied stresses and seasonal climatic (i.e., variant wetting) conditions. The H-VC behaviors of such soils are considered the main variables for designing these applications. However, in practice, examining such behaviors of expansive soils is usually considered under limited applied states.

In the last five decades, intensive studies have examined the behavior of expansive soils under cyclic wetting and drying (W/D) conditions in order to simulate climatic changes and environmental conditions [1–47]. Abbas et al. [47] presented a table that summarized the objectives and test conditions for previous research that investigated such behavior. The research interest in the cyclic W/D process applied to expansive soils lies in its implications for deformations, which may mainly distress the structures interacting with these layers. It can also alter their hydromechanical properties in a substantial manner compared to those estimated under common procedures that consider only the first wetting

condition. Undesirable estimation of such behavior may result in high costs, either pre-paid cost (during construction) or post-paid cost (during maintenance), of the relevant structures.

The volume change potential (VCP) under cyclic W/D shows different behavior responses. Some studies, e.g., [5,6,9,44,45,48], have concluded that this cyclic process results in cumulative swell strains, while others have shown swell fatigue (i.e., accumulated shrinkage), e.g., [1,3,4,8,13,24,32,36–38,47,49,50], and was explained as the soil particles exhibited continuous rearrangement, leading to a less active microstructure. The results of [12–14,34,44] reported both swell and shrinkage accumulation at the end of this cyclic process. Most of those research studies reported a reduction in swell accumulation and an increase in shrinkage accumulation as the applied stress increased. However, the majority of these studies investigated the VC behavior under cyclic W/D while considering small applied stresses, e.g., [5,7,44,45]. In order to mimic the applied stress conditions in the field, some researchers [1,11–14,24,32,37] studied that behavior for diverse stress conditions. However, the stress range for all of these studies was lower than the swell pressure (σ_s), inferring a swell potential for tested soils in the first wetting stage. In some engineering applications such as deep repositories, expansive soils are subjected to higher stress conditions, and VCP under cyclic W/D should be examined. Abbas et al. [47] investigated the VCP under cyclic W/D for a wide range of applied stresses to simulate probable loading conditions in the field.

In general, the main factors that affect the VC behavior are the clay particle percentage, expansive mineral content, initial placement condition, soil structure, current stress state, and stress history. However, at the end of the cyclic W/D process, the behavior of swell or shrinkage accumulation is attributed to the drying degree applied [12–14,34,44] or to the applied stress level and stress history of the soil [1,14,20,24,47,51]. Furthermore, almost all studies, except [14], reported an equilibrium elastic state for tested soils after several cycles of W/D that range between the third to fifth cycles. The largest drop in swell potential is noted in the first cycle [1,4,5,14,32,47], and [21] stated that the first cycle acts as a cycle that effectively reorients the soil structure from the primary placement condition to an equilibrium condition. Nevertheless, most studies dealing with cyclic W/D followed a sequence starting with the wetting cycle, except for [10], which started the process with the drying stage, while the onset of the environmental condition in the field may vary. In addition, no research has examined the influence of the onset phase of the W/D process on the VC behavior of expansive soils despite its probable variation in engineering practice.

In geotechnical engineering practice, saturated hydraulic conductivity (k_{sat}) is considered a key parameter for many projects. Generally, k_{sat} was deemed to be a constant for most soils. However, this hypothesis is invalid for clayey soils and, in particular, expansive clays. Numerous studies (e.g., [52–57]) showed that k_{sat} depends mainly on soil porosity, and several relationships were suggested to relate between the k_{sat} and the void ratio (e) [53,54,56–59]. In regard to the influence of cyclic W/D on such behavior, few studies were executed despite their practical importance.

The majority of these few studies, e.g., [29,60–62], reported an increase in k_{sat} with successive W/D cycles and imputed that to the developed cracks. Day [63] noted the same remark regarding the onset cycles; however, a reduction of the hydraulic conductivity is observed with further rewetting, which is ascribed to the expansive nature of clay promoting the completion of these desiccation cracks' healing. Albrecht and Benson [62] demonstrated the effect of stress state on crack healing and hence on k_{sat} upon successive W/D cycles.

Louati et al. [64] reported both an increase and a decrease in k_{sat} with repeated W/D cycles and referred that as the initial placement of samples. Micro-cracks are created during the drying process for dense, compacted specimens, while drying results in a diminution of the pores in the case of loosely compacted clay. Day [65] referred to the contradiction between former observations to the type of prevailing clay mineral. Dafalla et al. [50], and Albrecht and Benson [62] reported a reduction of k_{sat} with the application of surcharge, and [62] ascribed that to the increase in stress state, which helps in closing the cracks.

Abbas et al. [47] reported a general reduction trend of k_{sat} with successive W/D cycles for the wide range of applied stress examined and related this reduction to the noted accumulated shrinkage. In summary, k_{sat} change upon consecutive W/D cycles depends on the prevailing clay mineral, placement condition (water content and dry density), and stress state applied.

From the preceding discussion on both H-VC behaviors under cyclic W/D, it is noticed that the impact of the starting cycle of W/D on such behaviors is not considered in previous studies, while it is the most effective cycle and is responsible for soil fabric reorientation towards the equilibrium state. The main focus of the current research is to simulate the probable seasonal climatic variation under a wide range of stress conditions that most probably prevail in the field to obtain economical design procedures. The influence of the W/D onset cycle on H-VC behaviors is examined as well.

2. Material Used

The expansive soil investigated in the current study was collected as disturbed samples from a depth of 4.0 m below the ground surface from an open test pit that is located in the Iskan district of Al-Qatif city. This city is located along the shoreline of the Arabian Gulf coastal region of Saudi Arabia; see Figure 1.

Figure 1. Location map of Al-Qatif city.

A laser scattering particle size distribution analyzer was employed to obtain the particle size distribution curve of the investigated soil up to a clay size of 0.01 μm (Figure 2). It can be observed from Figure 2 that the selected soil comprises 1.0% fine sand, 32.0% silt, and 67.0% clay. The soil characterization results of Al-Qatif soil are summarized in Table 1. The collected expansive soil was classified as greenish-gray, extremely fissured, highly overconsolidated clay. Al-Qatif soil is a typical expansive soil encountered in the Arabian Gulf coastal region. It is derived from marl, calcareous limestone, and chert of the Tertiary and Quarternary ages, through the actions of geological and weathering processes [66], including glacial activity and successive transgression and regression cycles of gulf seawater that occurred during the late Pleistocene and Holocene ages [67,68].

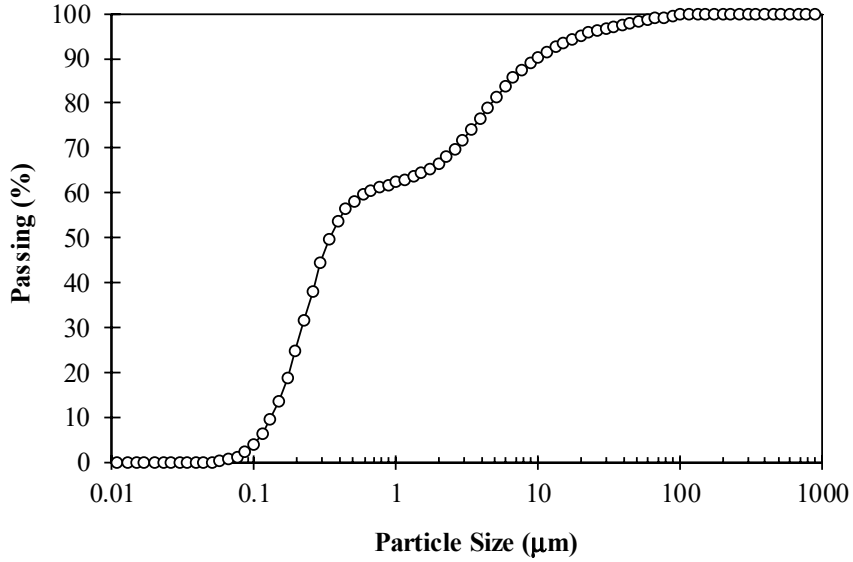

Figure 2. Particle size distribution of Al-Qatif soil.

Table 1. Characterization of Al-Qatif Clay.

Characteristic	Value
Specific gravity, G_S	2.72
Liquid limit, w_l (%)	137
Plastic limit, w_p (%)	45
Shrinkage limit, w_s (%)	20
Plasticity index, *PI* (%)	92
Unified soil classification system	CH [a]
Optimum moisture content, $w_{opt.}$ (%)	36
Maximum dry unit weight, γ_{dmax} (kN/m^3)	11.82

[a] CH refers to clay with high plasticity.

Former studies that were concerned with the mineralogical study of Al-Qatif's expansive soil [66,69–74] identified a high presence of smectite mineral based on X-ray diffraction (XRD) analysis. Chemical analysis was carried out using a 2.4 KW PANalytical AXIOS machine to determine the type and percentage of the oxides present in the specimens. Table 2 shows the elemental oxide composition for the tested material. The high percentage of SiO_2, Al_2O_3, MgO, Fe_2O_3, and CaO is indicative of the existence of smectite clay minerals, and therefore, the swell potential of the soil is most likely to be high. This is consistent with the findings from the XRD analysis.

Table 2. Chemical analysis of Al-Qatif soil.

Compound	Concentration
SiO_2	49.77
Al_2O_3	14.50
MgO	6.95
Fe_2O_3	6.36
K_2O	4.01
CaO	3.99
TiO_2	0.68
So_3	0.51
F	0.42
Na_2O	0.35
P_2O_5	0.22
Cl	0.18
LOI	11.83

3. Sample Preparation

For the sake of simulating engineered applications as well as minimizing heterogeneity in test results, compacted samples were used in the current experimental program. The collected samples were air-dried and pulverized to produce soil powder, which was mixed thoroughly with a target water content (w_c) of 32.0% and placed in plastic bags. The bags were stored in a humid desiccator for at least two days to ensure a uniform distribution of moisture. Afterward, the soil was compacted statically in oedometer rings (20.0 mm in height, and 50.0 mm internal diameter) to the target dry unit weight (γ_d) of 11.67 kN/m^3. The sample placement condition (i.e., w_c, and γ_d) was selected as 4% dry-of-optimum moisture content as obtained from a standard compaction test [75].

In order to estimate the as-compacted suction stress state, several specimens were prepared at the placeemnt condition, and the average value of as-compacted suction, which was 3.40 MPa, was obtained using a chilled-mirror dew point meter device (WP4C).

4. Testing Procedures and Equipment

The current experimental program consists of two series based on the onset stage of the W/D process, namely cyclic wetting and drying (CWD), which is adopted from Abbas et al. [47] (CS series), and cyclic drying and wetting (CDW). These two series simulate the potential environmental and seasonal climatic conditions in the field, and each of these series has included numerous tests that vary according to the applied axial wetting stress (σ_{aw}). In order to mimic the possible stress conditions in the field, four σ_{aw} values were considered in the current study, 25, 100, 300, and 1000 kPa, to display the behavior of the tested material for a diverse of VC conditions. Figure 3 depicts schematics for the stress/wetting paths followed in the CWD and CDW series.

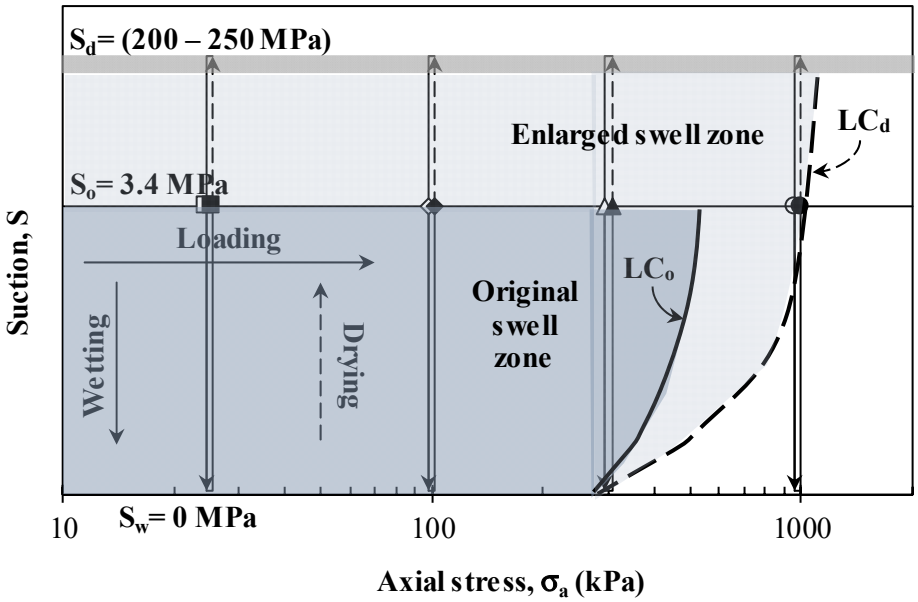

Figure 3. Executed stress paths and proposed load–collapse curves at as-compacted and dry states.

In order to evaluate the VCP under different stress conditions, oedometer testing (OED) was executed. Permeability testing was also adopted using the falling head technique, which was integrated into oedometer testing. After subjecting the tested specimen to the target stress condition according to Method B [76], it was subjected to five to six successive W/D cycles. In the case of CWD testing, the W/D process is initiated with the wetting stage, while in the case of CDW testing, the drying stage is started first. Generally, every stage was started after the former stage reached an equilibrium state with almost no variation in axial strain (ε_a) with time. The permeability stage was initiated after the wetting stage had ceased.

Two techniques for executing the W/D process were adopted in the literature: uncontrolled and controlled techniques. In uncontrolled techniques, the soaking and drying process were alternated, while the controlled cyclic wetting and drying process was achieved through adopting suction control. In the current experimental testing, the uncontrolled technique was adopted, where the wetting process was achieved through soaking, and drying was executed via air circulation during oedometer testing.

A fixed ring cell capable of implementing the falling head permeability test was utilized in this study to execute the oedometer testing. This facilitated the easy adoption of axial stress (σ_a) with accurate monitoring of axial deformation (Δh_a) and, hence, precise estimation of the void ratio (e). The oedometer cells were fitted with a linear variable differential transformer (LVDT) and connected to a datalogger. The permeability testing started with an approximate hydraulic head of 48 cm and stopped once four successive measurements of hydraulic conductivity led to the same value (±3%). A detailed description of the oedometer cell setup, with adjustments to execute permeability testing, in addition to the adoption of the W/D process is provided in [47].

The estimated average suction at the end of the drying cycles was measured using the WP4C device and found to range between 200 and 250 MPa.

5. Results and Discussions

This section presents the experimental program and depicts the effect of the starting stage of the W/D process and the applied stress condition on the H-VC behaviors of compacted highly expansive soil. The tabulated results of the executed testing program are provided in Table 3 (adopted from Abbas et al. [47]) and Table 4. It is aforementioned that positive values of ε_{ae} present swell potential, while negative values indicate collapse potential.

Table 3. Test conditions and results of CWD series.

Sample ID	Wetting Stress	Equilibrium Axial Strain, e_{ae} (%)												Sat. Hydr. Conduct., k_{sat} ($\times 10^{-7}$ cm/s.)					
	s_{aw} (kN/m^2)	1st Cycle		2nd Cycle		3rd Cycle		4th Cycle		5th Cycle		6th Cycle		1st Cycle	2nd Cycle	3rd Cycle	4th Cycle	5th Cycle	6th Cycle
		W	D	W	D	W	D	W	D	W	D	W	D						
CWD_25	25	15.5	−1.9	13.2	−1.4	11.0	−2.7	8.7	−3.5	8.3	−5.4	7.5	−6.2	5.4	5.0	4.2	4.6	3.4	2.8
CWD_100	100	8.0	−6.0	3.7	−8.8	1.13	−10	−0.5	−12	−1.7	−13	−2.7	−13	2.2	1.9	1.6	1.3	1.2	0.9
CWD_300	300	−0.2	−15	−7.2	−19	−9.6	−20	−11	−22	−12	−22	−13	−23	0.6	0.5	0.4	0.4	0.4	0.4
CWD_1000	1000	−8.4	−25	−17	−27	−19	−29	−20	−30	−21	−31	−22	−31	0.2	0.1	0.2	0.1	0.1	0.1

Table 4. Test conditions and results of CDW series.

Sample ID	Wetting Stress	Equilibrium Axial Strain, ε_{ae} (%)												Sat. Hydr. Conduct., k_{sat} ($\times 10^{-7}$ cm/s.)					
	σ_{aw} (kN/m^2)	1st Cycle		2nd Cycle		3rd Cycle		4th Cycle		5th Cycle		6th Cycle		1st Cycle	2nd Cycle	3rd Cycle	4th Cycle	5th Cycle	6th Cycle
		W	D	W	D	W	D	W	D	W	D	W	D						
CDW_25	25	−3.0	18.7	2.9	16.4	2.6	14.3	2.2	13.1	1.7	12.3			10.1	6.0	5.2	5.2	4.6	
CDW_100	100	−6.5	4.2	−10.3	−0.4	−12.5	−3.0	−14.4	−4.7	−16.3	−5.9			2.3	1.0	1.0	0.9	0.9	
CDW_300	300	−5.7	−1.6	−11.1	−6.3	−14.8	−8.4	−17.0	−9.8	−18.8	−10.8	−19.8	−11.6	0.9	0.4	0.4	0.4	0.3	0.3
CDW_1000	1000	−10.8	−11.0	−20.6	−17.6	−21.2	−18.0	−21.5	−18.8	−21.6	−19.5	−21.7	−20.0	0.3	0.2	0.2	0.2	0.1	0.1

5.1. Volume Change Behavior during First Wetting Stage

The VCP for the first wetting stage of both executed series, i.e., CWD and CDW series, is depicted in the form of variations of strain states (either swell or collapse) versus time

(t), as shown in Figure 4a–d. Regarding CWD testing, three trends for (ε_{aw}-t) relations, namely swell, swell–collapse, and collapse, were observed depending on the applied σ_{aw}. Specifically, swell potential was observed for samples CWD_25 and CWD_100, as shown in Figure 4a,b, while collapse potential was observed for samples labeled CWD_1000. Sample CWD_300 exhibited swell behavior in the early portion of the test followed by collapse. Similarly, the same three trends of (ε_{aw}-t) relations were observed for the CDW series, but with different values of axial wetting strain (ε_{aw}) under the same σ_{aw}. Figure 4a,b show that both CDW_25 and CDW_100 exhibited a swell potential at the first wetting stage after the onset drying stage, however, with different values of ε_{aw} compared with those of CWD_25 and CWD_100, respectively. Figure 4c shows a swell–collapse behavior for CDW_300, similar to CWD_300; however, it exhibited a final swell potential in contrast to CWD_300, which exhibited final collapse. Figure 4d shows that specimen CDW_1000 exhibited a swell–collapse behavior, in contrast to CWD_1000, which exhibited collapse potential.

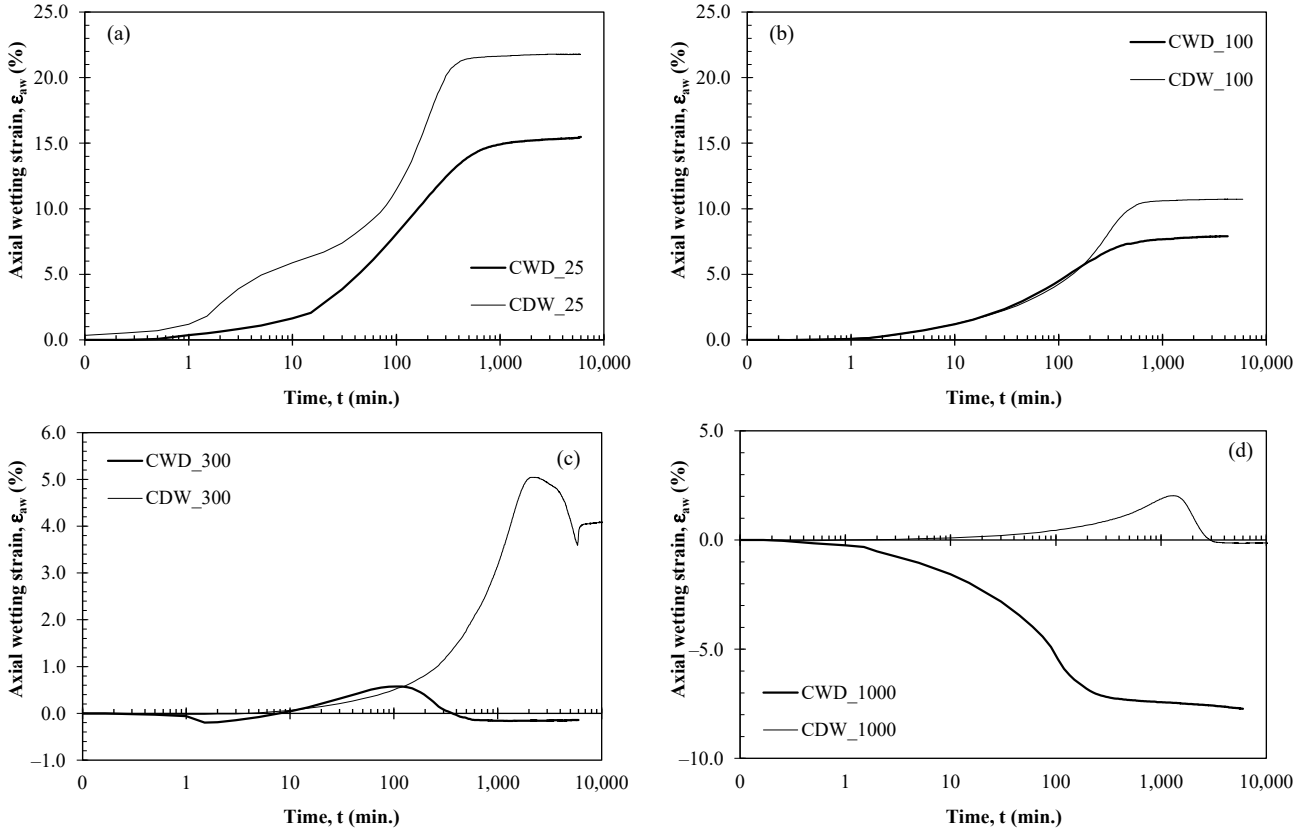

Figure 4. (ε_{aw}-t) during the first wetting stage of CWD and CDW series for σ_{aw}: (**a**) 25 kPa, (**b**) 100 kPa, (**c**) 300 kPa, and (**d**) 1000 kPa.

Several constitutive models have been proposed to describe the behavior of expansive soils. The Barcelona Expansive Model (BExM) is considered one of the pioneering and succeesful models to describe the elasto-plastic behavior of expansive soils. A conceptual basis for this model is described in [77], while the full mathematical formulation of the model is presented in [78]. The core of the BExM model is the yield curve that separates the elastic from the plastic behavior and is postulated to uniquely represent both wetting and stress-induced yield points. Gens and Alonso [77], and subsequently [4,78], proposed to represent the yield locus, for the case of oedometer tests (i.e., one-dimensional loading condition), either in the ($\sigma_a - s$) or ($p - s$) plane by the load–collapse (LC) curve. The plastic hardening associated with subjecting the expansive soil specimen to stresses (either loading or suction) greater than its past stress history resulted in an enlargement of the load–collapse (LC) curve.

The observed behavior in the preceding section can be interpreted using the yield curve concept (i.e., LC curve) developed within the Barcelona Expansive Model (BExM). A plot of the LC curve boundaries for the tested soil, which defines the swell zones is shown in Figure 3. The boundaries of LC were determined using the two yield points: at zero suction (σ_o*) and at pre-wetting suction (σ_o). The yield stress at zero suction (σ_o*) was obtained as the axial stress at the equilibrium state attained at the end of wetting under constant volume condition. However, the yield stress at pre-wetting suction (σ_o) was estimated based on Casagrande's method, as obtained from the loading curve at pre-wetting suction. As mentioned formerly, the LC curve is assumed to characterize the wetting-induced yield points, i.e., the start of collapse behavior. However, this yield curve is related to the pre-wetting state of the tested specimen. For specimens tested in the CWD series, the pre-wetting state is its as-compacted state, while the pre-wetting state of the CDW series is its state at the end of the first drying stage. The boundaries of the load–collapse curve for the CWD series (LC_o), i.e., at the as-compacted state, are determined in the stress range of 237–500 kPa.

Regarding wetting from the as-compacted state, LC_o curve bounds the original swell zone, the dark shaded zone in Figure 3. Specimens labeled CWD_25 and CWD_100 ($\sigma_{aw} < \sigma_o$* = 237 kPa), which are wetted from their as-compacted state, experienced swell behavior, while those under application of stress exceeding the yield stress at as-compacted suction ($\sigma_{aw} > \sigma_o$ = 500 kPa) underwent collapse behavior, such as the CWD_1000 test. A swell–collapse behavior was observed for wetting paths of samples under constant stress ranging between 237 and 500 kPa, such as the CWD_300 test.

With respect to the CDW specimens, the drying stage that initiated from the as-compacted state resulted in a denser structure of the tested specimens, as a result of the shrinkage during drying. Hence, it is expected to exhibit a higher value of the yield stress at the dry state, or in other words, an enlargement of the load–collapse curve to its dry load–collapse (LC_d) curve as proposed in Figure 3. So, the initial drying resulted in an enlargement of the swell zone, as distinguished by the light shaded zone shown in Figure 3. The observed behavior of the CDW_25 and CDW_100 tests reinforces the enlargement of the swell zone, where these specimens exhibited more swell compared to those wetted from the as-compacted state, as shown in Figure 4a,b. Additionally, the CDW_300 test exhibited a swell–collapse behavior, but with higher swell compared to CWD_300. Finally, the test labeled CDW_1000 showed a swell–collapse behavior, as shown in Figure 4d, unlike the CWD_1000 test, which is evidence of the enlargement of the LC curve and the swell zone.

5.2. Impact of Cyclic Wetting and Drying on Volume Change Behavior

The VCP of samples subjected to the W/D process is presented in the form of a trend of variation in the equilibrium axial strain (ε_{ae}) for consecutive W/D cycles, as shown in Figure 5a as a typical plot. This plot is considered a summary of the variation in ε_{aw} at the equilibrium state of the wetting or drying stage (Figure 5b). The ε_{ae} is defined as the percentage of axial deformation (Δh_a) of the sample at equilibrium during either wetting or drying with respect to the original height (h_i) of the sample prior to initial wetting or drying.

Figure 6a–d exhibit the trend of variation in the ε_{ae} for consecutive W/D cycles for both the CWD and CDW series. An accumulated shrinkage strain is detected for all tested samples of both series, either experiencing swell, swell–collapse, or collapse potential during the first wetting stage. This agrees with the results of [1,4,8,13,24,32,36–38,47,49,50]. The observed accumulated shrinkage strain is related to the initial compacted state (lightly compacted) as suggested in [7]. Furthermore, both tested series achieved an elastic response (i.e., equilibrium condition) through the repeated W/D cycles.

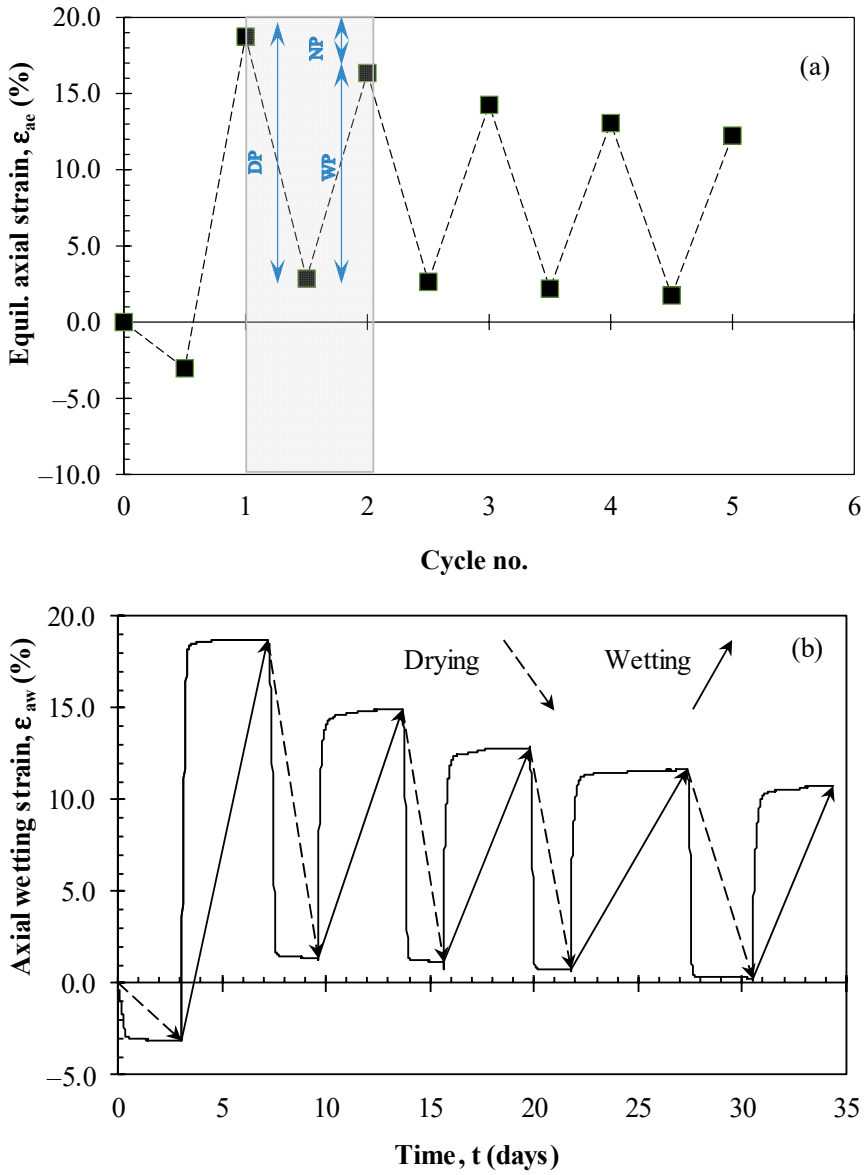

Figure 5. Typical trend of variation in (**a**) ε_{ae}—cycle no. and (**b**) ε_{ae}—time for W/D cycles.

To better clarify the observed results, two parameters are concluded from the variation trend of ε_{ae} with successive W/D cycles: wetting potential (WP, %) and drying potential (DP, %), as shown in the second cycle of the typical (ε_{ae}–cycle no.) plot (shaded zone in Figure 5a). These parameters represent the VCP attained at each stage of the repeated cycles. The plastic axial strain attained at the end of each cycle is represented by the difference between these two parameters, i.e., the net axial strain after each cycle (NP, %). As mentioned before, negative values of NP represent shrinkage accumulation.

Figures 7–9 compare between the evolution of WP, DP, and NP, respectively, with successive W/D cycles for both the CWD and CDW series. Except for the first cycle, the WP of the CDW series is generally lower than that of CWD. Moreover, an elastic response (equilibrium condition) to the wetting process is attained starting in the fourth to fifth cycle for both series. The difference between the WP of both the CWD and CDW series at their equilibrium value increases as the σ_{aw} increases. These observations suggest a recommendation for the construction aspects of subjecting the compacted layers to a drying process to eliminate the wetting potential of compacted expansive soil, especially for applications with higher applied stress.

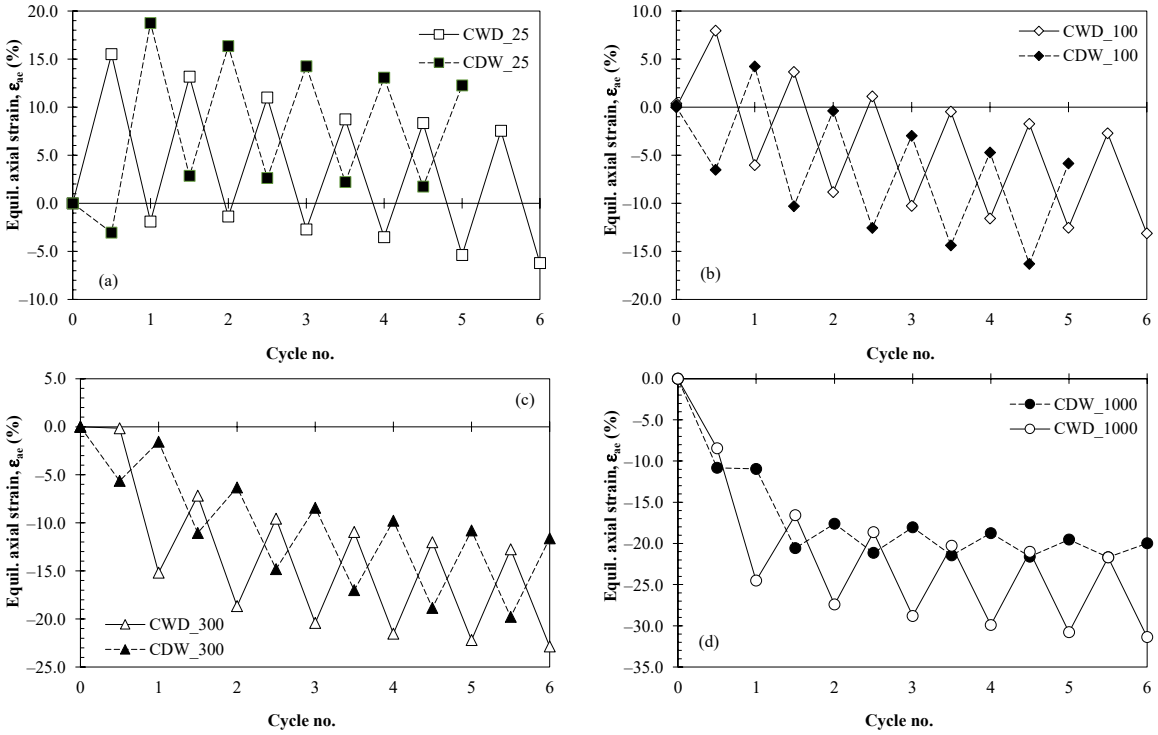

Figure 6. Evolution of VCP with W/D cycles for CWD and CDW series for σ_{aw}: (**a**) 25 kPa, (**b**) 100 kPa, (**c**) 300 kPa, and (**d**) 1000 kPa.

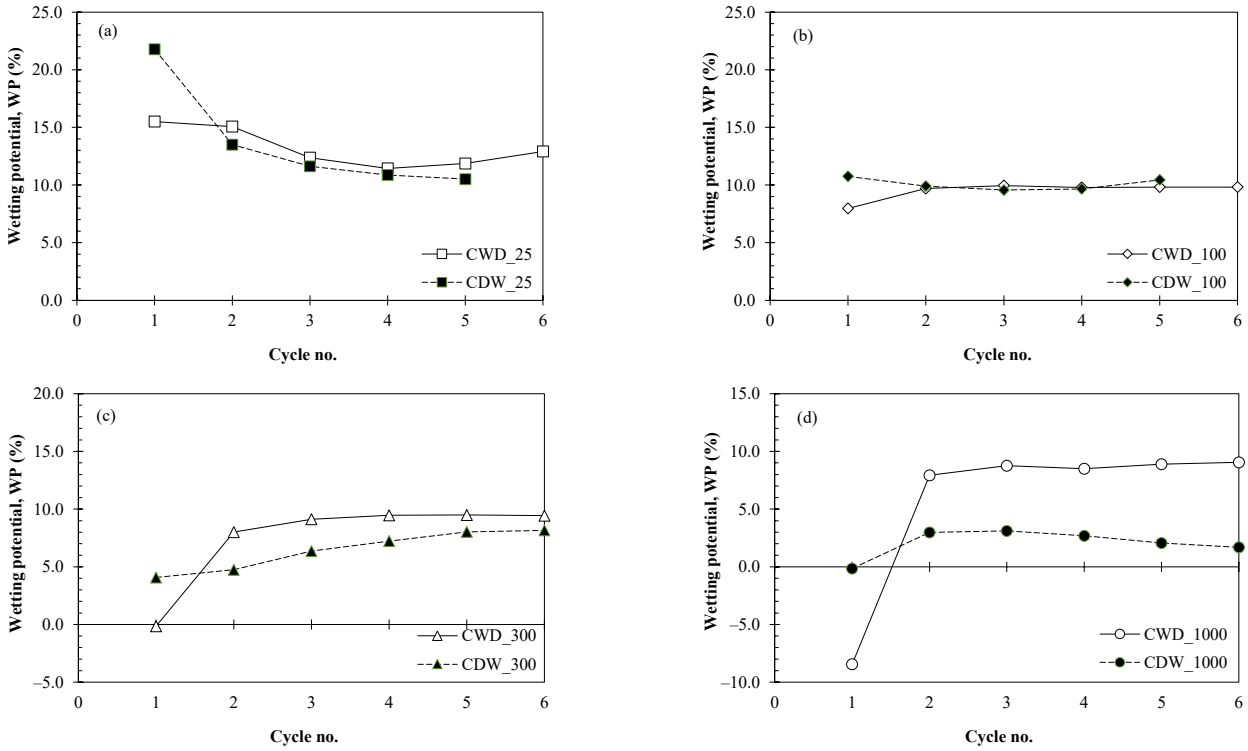

Figure 7. Variations in WP with consecutive W/D cycles for CWD and CDW series for σ_{aw}: (**a**) 25 kPa, (**b**) 100 kPa, (**c**) 300 kPa, and (**d**) 1000 kPa.

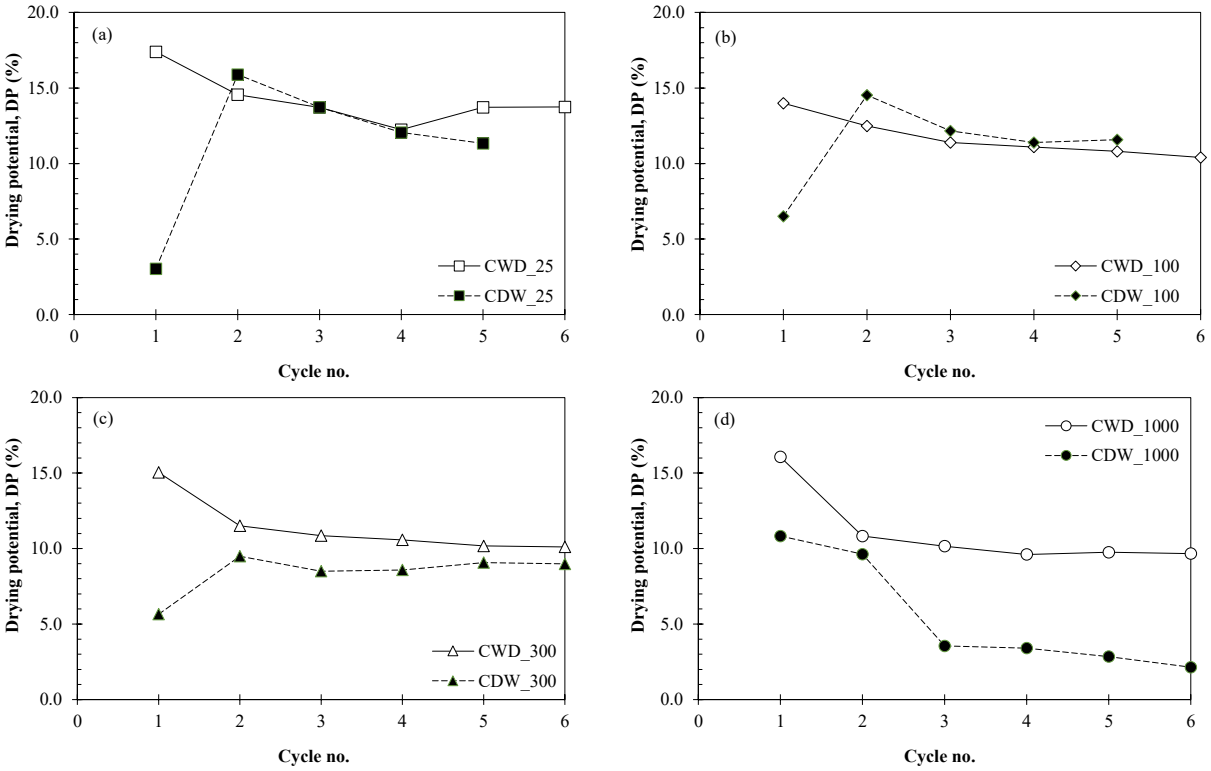

Figure 8. Variations in DP with consecutive W/D cycles for CWD and CDW series for σ_{aw}: (**a**) 25 kPa, (**b**) 100 kPa, (**c**) 300 kPa, and (**d**) 1000 kPa.

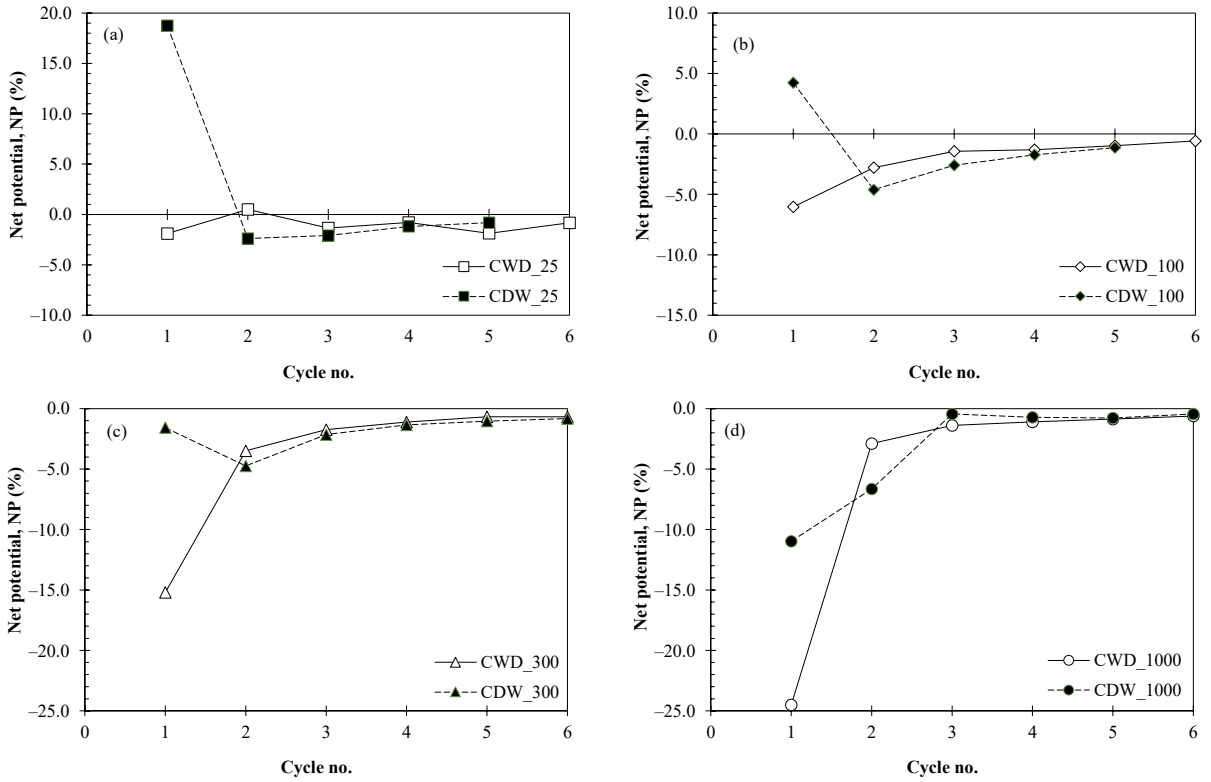

Figure 9. Variations in NP with consecutive W/D cycles for CWD and CDW series for σ_{aw}: (**a**) 25 kPa, (**b**) 100 kPa, (**c**) 300 kPa, and (**d**) 1000 kPa.

Figure 8a–d show that the DP of the CDW series is generally lower than that of CWD and reaches its equilibrium values starting from the fourth cycle. The plastic strains attained at the close of each cycle are represented in Figure 9a–d in terms of the NP evolution with W/D advance. Starting from the cycle of equilibrium (i.e., almost the fourth cycle), NP for both tested series shows an almost identical trend with small values of accumulated shrinkage.

The variation in swell potential with applied stress is an important trend and can be represented by the (WP-σ_{aw}) function. Figure 10a,b depict the progress of the (WP-σ_{aw}) trend with consecutive W/D cycles for both the CWD and CDW series, respectively. It is evident from Figure 10a,b that the (WP-σ_a) functions of both series show less response to applied stress with development of W/D cycles. A unique trend is attained for each series starting from the third cycle.

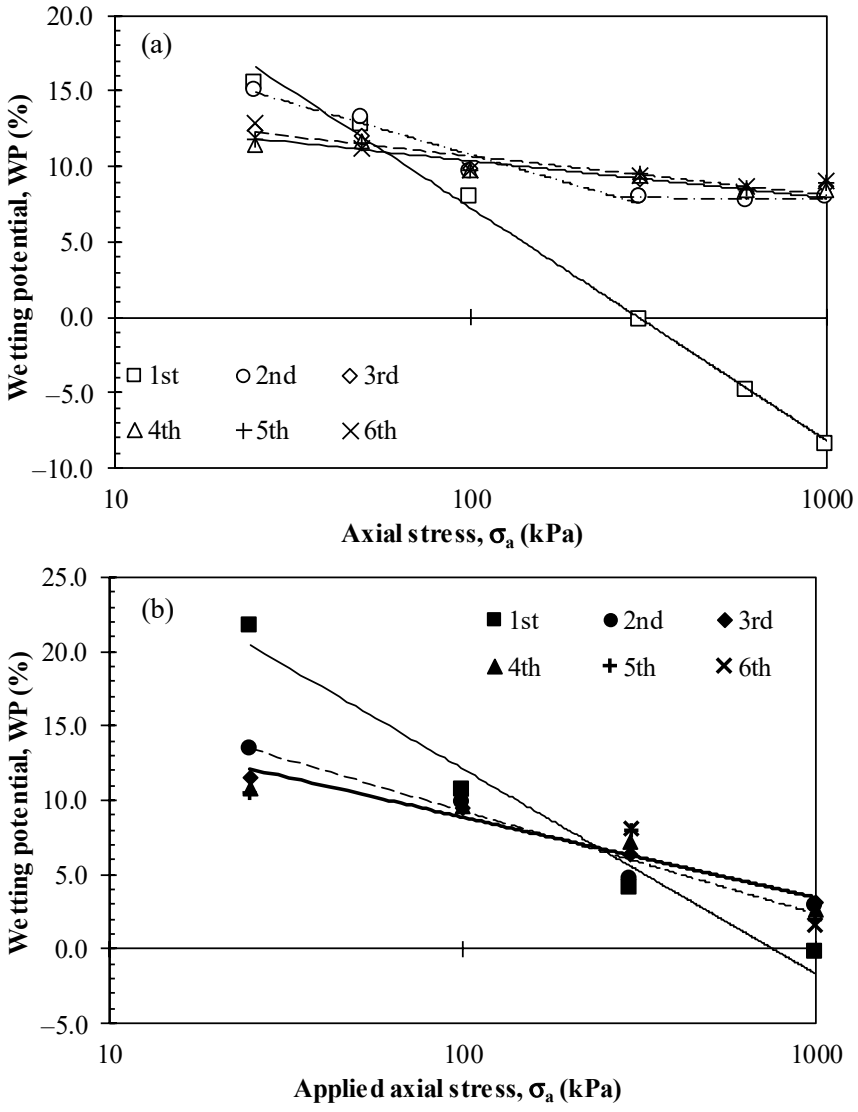

Figure 10. (WP−σ_a) relations for consecutive W/D cycles of (**a**) CWD and (**b**) CDW series.

To better understand VC behavior, plots of trend of variation in the post-wetting void ratio (e_w) versus σ_{aw}, marked for expansive soils, for sequential wetting cycles are presented for CWD and CDW in Figure 11a,b. The accumulated shrinkage of the void ratio with the W/D process is noted for both series. Moreover, the (e_w-log σ_{aw}) relation is valid for all cycles exhibiting an equilibrium condition as the W/D process progresses.

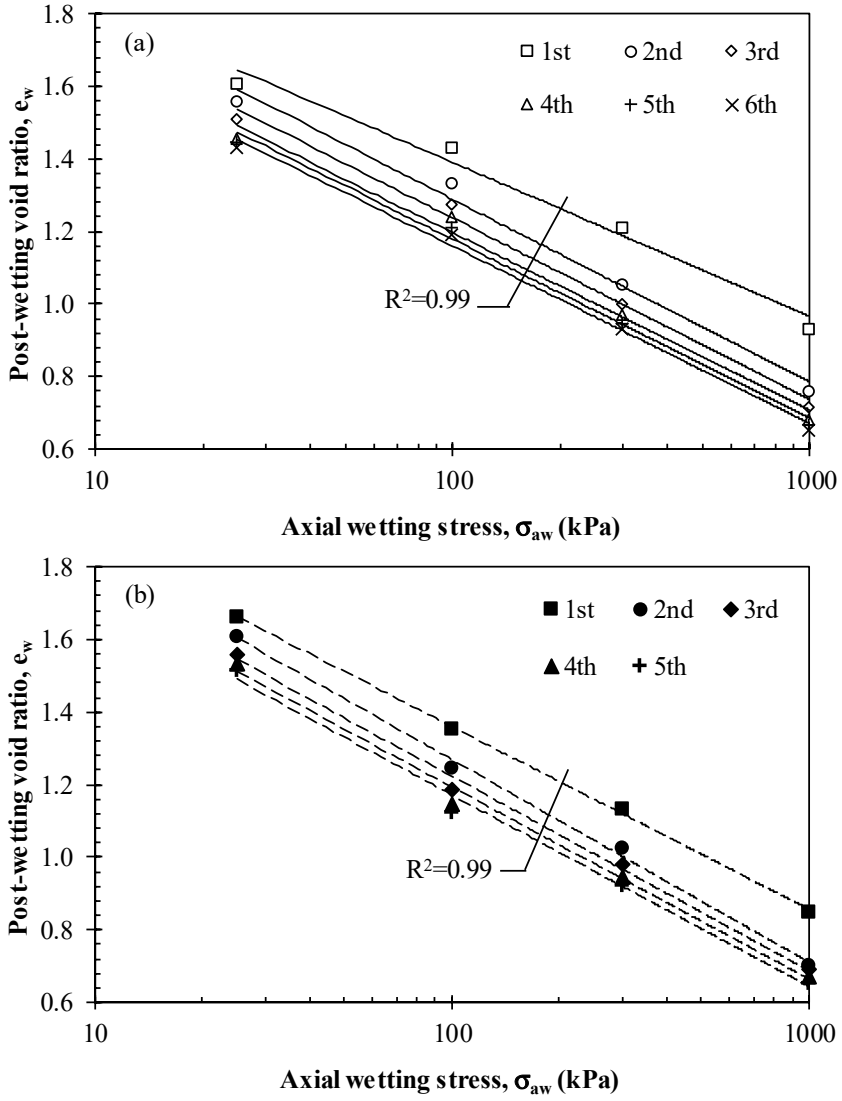

Figure 11. (e_w-σ_a) relations for consecutive W/D cycles of (**a**) CWD and (**b**) CDW series.

5.3. Impact of Cyclic Wetting and Drying on Hydraulic Conductivity

Figure 12a–d show the variation in k_{sat} with the successive W/D process for both the CWD and CDW series. A reduction in k_{sat} with an advance in the W/D process is observed for both series under all the stress states applied. This is attributed to the shrinkage accumulation noted during repeated W/D cycles, which results in a reduction of the post-wetting void ratio (e_w). This observation is contrary to previous studies (e.g., [29,60–62]) that reported an increase in k_{sat} with successive W/D cycles. This contrast may be attributed to the partial recovery of drying cracks, which is reported in some of those studies, while in the current study, the high percentage of montmorillonite clay in the tested soil is responsible for the full healing of cracks developed during drying. For each applied stress state, comparable results of k_{sat} for both series are noted, except for the first wetting cycle. Moreover, an equilibrium condition for k_{sat} is attained from the third cycle for almost all tests.

Figure 13a,b show that the k_{sat} is inversely correlated to the applied axial stress (σ_a), with an observed impact of the applied W/D process on the trends for both the CWD and CDW series. These inverse relationships (k_{sat}-σ_a) are related to the reduction of e_w associated with increasing σ_a as reported by many researchers. In this regard, k_{sat} is plotted as a function of e_w for both the CWD and CDW series, in Figures 14 and 15, respectively. For both series, the relationship (k_{sat}-e_w) showed highly correlated individual trends for the first, second, and third to fifth cycles. Figure 16 compiles the data for both series to

show the impact of the W/D order on hydraulic behavior. It is evident from Figure 16a that the k_{sat} for the CDW series is higher than that of CWD for the first cycle of W/D. This can be attributed to probable minor cracks that may be developed during the first drying cycle that initiated the CDW testing. Comparable (k_{sat}-e_w) trends for both series are noted in Figure 16b for the second cycle. A unique strongly correlated trend for both series is depicted in Figure 16c for the results from the third to fifth cycles. This infers the role that repetitive wetting cycles play in crack healing and hence diminishes any effect of the onset stage of the W/D process. Accordingly, exposing compacted expansive soil layers in the field to repetitive W/D cycles resulted in acquiring a steady state for the k_{sat} that is independent of its previous wetting history.

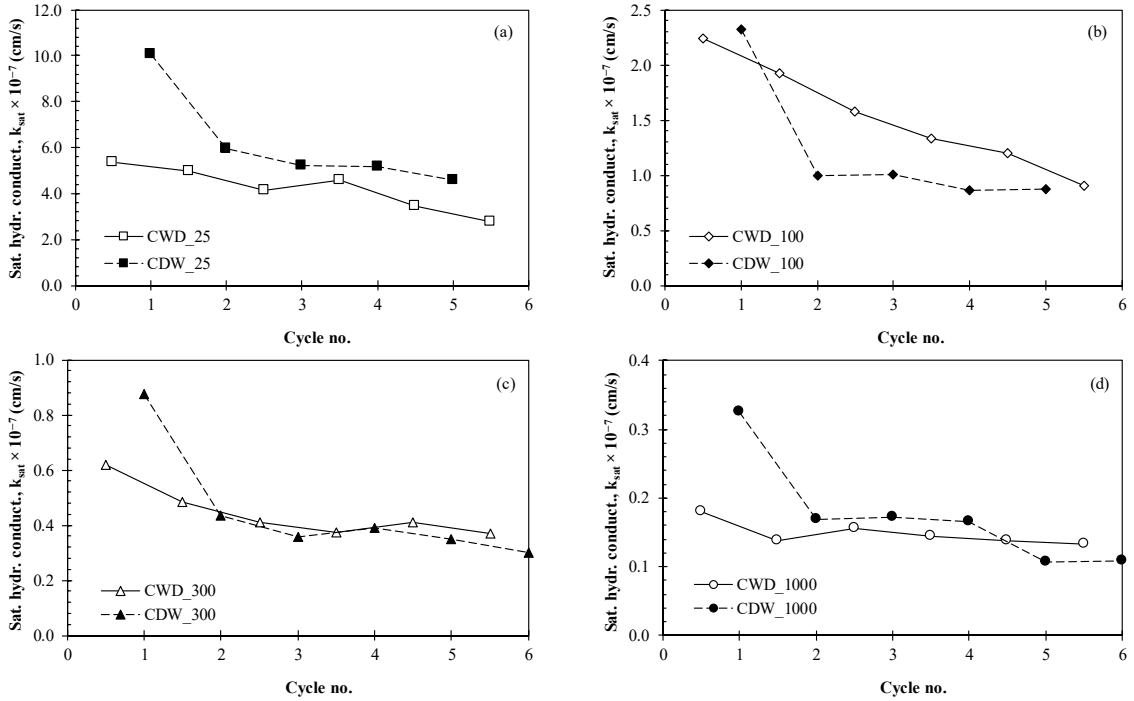

Figure 12. Variations of k_{sat} with consecutive W/D cycles for CWD and CDW series for σ_{aw}: (**a**) 25 kPa, (**b**) 100 kPa, (**c**) 300 kPa, and (**d**) 1000 kPa.

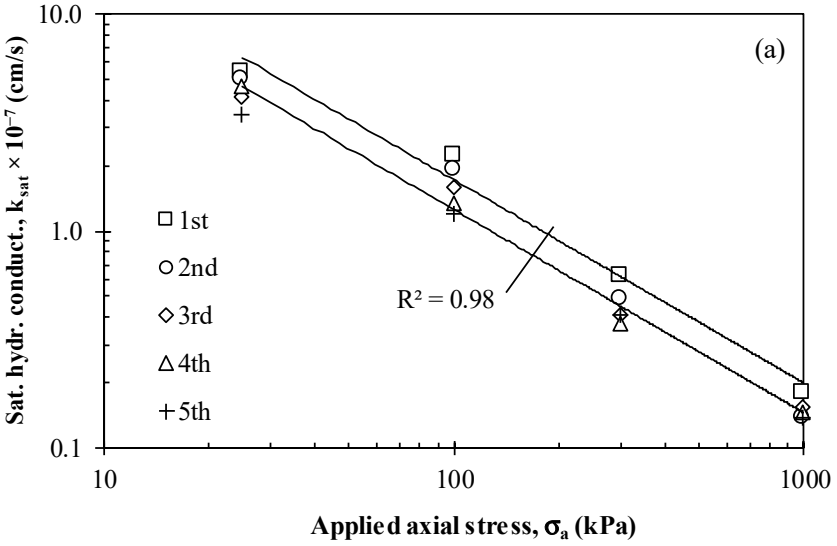

Figure 13. *Cont.*

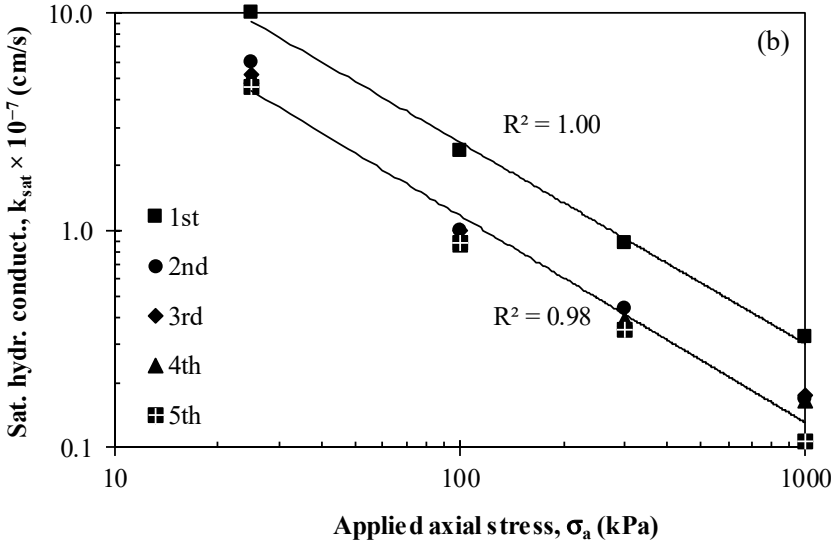

Figure 13. (k_{sat}-σ_a) relations for consecutive W/D cycles of (**a**) CWD and (**b**) CDW series.

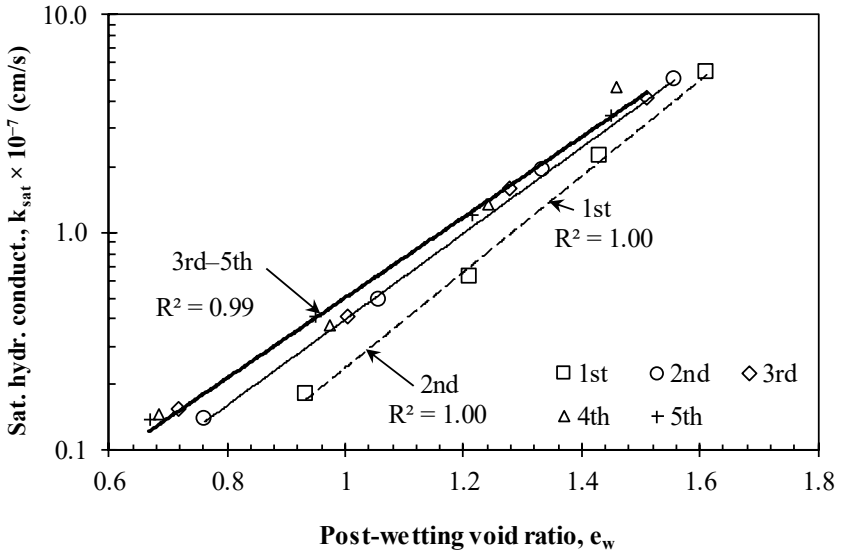

Figure 14. (k_{sat}-e_w) functions for CWD series.

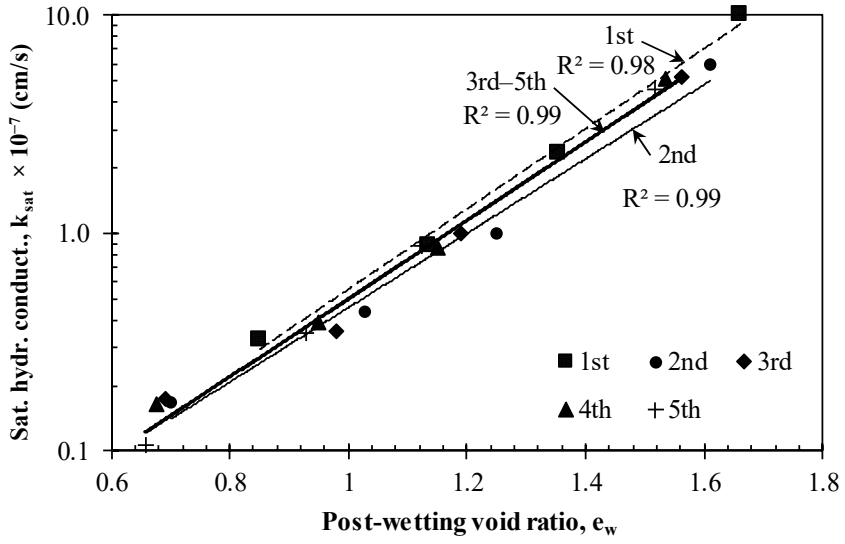

Figure 15. (k_{sat}-e_w) functions for CDW series.

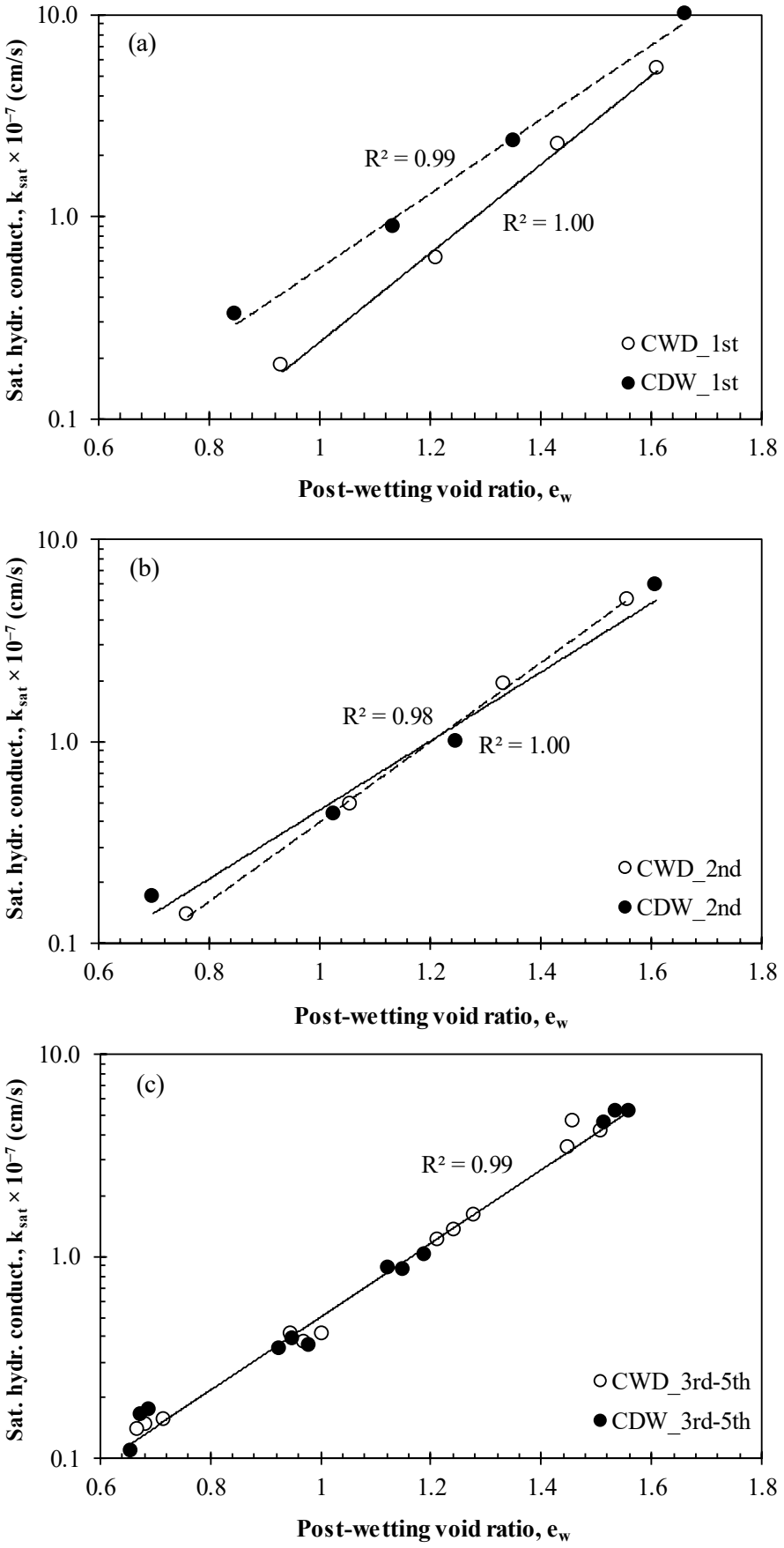

Figure 16. Comparison between (k_{sat}-e_w) functions of CWD and CDW series for: (**a**) 1st cycle, (**b**) 2nd cycle, and (**c**) 3rd–4th cycles.

6. Conclusions

This study involved simulating the effects of probable field stress and seasonal climatic variations on the H-VC behaviors of Al-Qatif's expansive soils. The impact of the starting stage of the W/D process on such behaviors was studied through implementing two series of cyclic W/D processes, CWD and CDW, for various axial stress states. Based on the current study results, it is inferred that:

1. The observed VCP during the first wetting stage of both tested series was interpreted using the yield curve concept (LC curve) developed within the BExM model, with evidence of its enlargement as the tested sample was subjected to stresses (i.e., suction) greater than its previous stress history.
2. The cyclic W/D process adopted, either CWD or CDW, has an impact on the H-VC behaviors of expansive soils, with the first cycle of wetting and drying being the most effective cycle for effectively reorienting the soil fabric towards an equilibrium state.
3. Swell fatigue, experienced as accumulated shrinkage, was reported for both testing series, and this behavior was attributed to the initial placement condition, specified as a loose compacted state.
4. An elastic response to the W/D process is achieved in the third to fourth cycle for both tested series in terms of H-VC behaviors.
5. The onset stage of the W/D affects the WP, where its values were generally lower for CDW than those of CWD. The difference between the values of both series at their equilibrium value increased as the σ_{aw} increased. A recommendation of subjecting the compacted layers to a drying process is suggested to eliminate the wetting potential of the compacted expansive soil.
6. A reduction trend of k_{sat} with an advance in the W/D process is reported for both series under all the applied stress states, which is attributed to the accumulated shrinkage noted during repeated W/D cycles.
7. A unique (k_{sat}-e_w) correlation that combines both series' results starting from the third cycle is observed, while the first cycle showed higher values of k_{sat} for the W/D process started with drying. Consequently, it is recommended to submerge the compacted clay barrier after its construction to obtain a barrier with the lowest values of hydraulic conductivity.

Funding: This research was funded by the Deputyship for Research & Innovation, Ministry of Education in Saudi Arabia, grant number [IF2/PSAU/2022/01/23040].

Institutional Review Board Statement: Not applicable.

Informed Consent Statement: Not applicable.

Data Availability Statement: All data generated or used during the study appear in the submitted article.

Acknowledgments: The authors extend their appreciation to the Deputyship for Research & Innovation, Ministry of Education in Saudi Arabia for funding this research work through the project number (IF2/PSAU/2022/01/23040). The author is grateful to Eng. Abdullah Bugshan Research Chair in Expansive Soils and Geotechnical Laboratory, Civil Engineering Department, King Saud University for supporting the research through providing access to their facilities.

Conflicts of Interest: The author declares no conflict of interest.

Nomenclature

γ_d	Dry unit weight
w_c	Water content
σ_a	Applied axial stress
σ_o	Yield stress at pre-wetting suction
σ_o*	Yield stress at saturation
H-VC	Hydraulic and volume change
LC	Load-collapse curve
σ_{aw}	Axial wetting stress
ε_{aw}	Axial wetting strain
ε_{ae}	Equilibrium axial strain
W/D	Wetting and drying
CWD	Cyclic wetting and drying
CDW	Cyclic dying and wetting
WP	Wetting potential
DP	Drying potential
NP	net axial strain
VCP	Volume change potential
e_w	Post-wetting void ratio
k_{sat}	Saturated hydraulic conductivity

References

1. Al-Homoud, A.S.; Basma, A.A.; Husein Malkawi, A.I.; Al Bashabsheh, M.A. Cyclic Swelling Behavior of Clays. *J. Geotech. Eng.* **1995**, *121*, 562–565. [CrossRef]
2. Basma, A.A.; Al-Homoud, A.S.; Husein, A. Laboratory Assessment of Swelling Pressure of Expansive Soils. *Appl. Clay Sci.* **1995**, *9*, 355–368. [CrossRef]
3. Basma, A.A.; Al-Homoud, A.S.; Husein Malkawi, A.I.; Al-Bashabsheh, M.A. Swelling-Shrinkage Behavior of Natural Expansive Clays. *Appl. Clay Sci.* **1996**, *11*, 211–227. [CrossRef]
4. Alonso, E.E.; Romero, E.; Hoffmann, C.; García-Escudero, E. Expansive Bentonite-Sand Mixtures in Cyclic Controlled-Suction Drying and Wetting. *Eng. Geol.* **2005**, *81*, 213–226. [CrossRef]
5. Estabragh, A.R.; Parsaei, B.; Javadi, A.A. Laboratory Investigation of the Effect of Cyclic Wetting and Drying on the Behaviour of an Expansive Soil. *Soils Found.* **2015**, *55*, 304–314. [CrossRef]
6. Nowamooz, H.; Mrad, M.; Abdallah, A.; Masrouri, F. Experimental and Numerical Studies of the Hydromechanical Behaviour of a Natural Unsaturated Swelling Soil. *Can. Geotech. J.* **2009**, *46*, 393–410. [CrossRef]
7. Nowamooz, H.; Masrouri, F. Mechanical Behaviour of Expansive Soils after Several Drying and Wetting Cycles. *Geomech. Geoeng.* **2010**, *5*, 213–221. [CrossRef]
8. Day, R.W. Swell-Shrink Behavior of Compacted Clay. *J. Geotech. Geoenviron. Eng. ASCE* **1994**, *120*, 618–623. [CrossRef]
9. Estabragh, A.R.; Moghadas, M.; Javadi, A.A. Effect of Different Types of Wetting Fluids on the Behaviour of Expansive Soil during Wetting and Drying. *Soils Found.* **2013**, *53*, 617–627. [CrossRef]
10. Estabragh, A.R.; Moghadas, M.; Javadi, A.A. Mechanical Behaviour of an Expansive Clay Mixture during Cycles of Wetting and Drying Inundated with Different Quality of Water. *Eur. J. Environ. Civ. Eng.* **2015**, *19*, 278–289. [CrossRef]
11. Wheeler, S.J.; Sharma, R.S.; Buisson, M.S.R. Coupling of Hydraulic Hysteresis and Stress–Strain Behaviour in Unsaturated Soils. *Géotechnique* **2003**, *53*, 41–54. [CrossRef]
12. Farulla, C.A.; Ferrari, A.; Romero, E. *Mechanical Behaviour of Compacted Scaly Clay during Cyclic Controlled-Suction Testing in Experimental Unsaturated Soil Mechanics*; Springer Proceedings in Physics; Springer: Berlin/Heidelberg, Germany, 2007; Volume 112, ISBN 0008-3674.
13. Airò Farulla, C.; Ferrari, A.; Romero, E. Volume Change Behaviour of a Compacted Scaly Clay during Cyclic Suction Changes. *Can. Geotech. J.* **2010**, *47*, 688–703. [CrossRef]
14. Zemenu, G.; Martine, A.; Roger, C. Analysis of the Behaviour of a Natural Expansive Soil under Cyclic Drying and Wetting. *Bull. Eng. Geol. Environ.* **2009**, *68*, 421–436. [CrossRef]
15. Dong, J.G.; Xu, G.Y.; Lv, H.B.; Yang, J.Y. An Instrument for Wetting-Drying Cycle of Expansive Soil under Simulated Loads and Experimental Research. *J. Eng. Res.* **2019**, *7*, 1–12.
16. Yazdandoust, F.; Yasrobi, S.S. Effect of Cyclic Wetting and Drying on Swelling Behavior of Polymer-Stabilized Expansive Clays. *Appl. Clay Sci.* **2010**, *50*, 461–468. [CrossRef]
17. Sajedi, K.; Huat, B.B.K.; Bazaz, J.B. Effects of Cyclic Test in Decreasing Damages to Structures and Roads on Gypsum Soils. In Proceedings of the 6th International Conference on Case Histories in Geotechnical Engineering, Chicago, IL, USA, 11–16 August 2008; pp. 1–10.

18. Allam, M.M.; Sridharan, A. Effect of Wetting and Drying on Shear Strength. *J. Geotech. Eng. Div. ASCE* **1981**, *107*, 421–438. [CrossRef]
19. Doostmohammadi, R.; Moosavi, M.; Mutschler, T.; Osan, C. Influence of Cyclic Wetting and Drying on Swelling Behavior of Mudstone in South West of Iran. *Environ. Geol.* **2009**, *58*, 999–1009. [CrossRef]
20. Guney, Y.; Sari, D.; Cetin, M.; Tuncan, M. Impact of Cyclic Wetting-Drying on Swelling Behavior of Lime-Stabilized Soil. *Build. Environ.* **2007**, *42*, 681–688. [CrossRef]
21. Rosenbalm, D.; Zapata, C.E. Effect of Wetting and Drying Cycles on the Behavior of Compacted Expansive Soils. *J. Mater. Civ. Eng.* **2017**, *29*, 04016191. [CrossRef]
22. Tripathy, S.; Rao, K.S.; Fredlund, D.G. Water Content-Void Ratio Swell-Shrink Paths of Compacted Expansive Soils. *Can. Geotech. J.* **2002**, *39*, 938–959. [CrossRef]
23. Tripathy, S.; Subba Rao, K.S. Cyclic Swell-Shrink Behaviour of a Compacted Expansive Soil. *Geotech. Geol. Eng.* **2009**, *27*, 89–103. [CrossRef]
24. Baille, W.; Tripathy, S.; Schanz, T. Swelling Pressures and One-Dimensional Compressibility Behaviour of Bentonite at Large Pressures. *Appl. Clay Sci.* **2010**, *48*, 324–333. [CrossRef]
25. Hanafy, E.D.E. Swelling/Shrinkage Characteristic Curve of Desiccated Expansive Clays. *Geotech. Test. J.* **1991**, *14*, 206–211. [CrossRef]
26. Krisdani, H.; Rahardjo, H.; Leong, E.C. Effects of Different Drying Rates on Shrinkage Characteristics of a Residual Soil and Soil Mixtures. *Eng. Geol.* **2008**, *102*, 31–37. [CrossRef]
27. Wang, G.; Wei, X. Modeling Swelling–Shrinkage Behavior of Compacted Expansive Soils during Wetting–Drying Cycles. *Can. Geotech. J.* **2015**, *52*, 783–794. [CrossRef]
28. Julina, M.; Thyagaraj, T. Combined Effects of Wet-Dry Cycles and Interacting Fluid on Desiccation Cracks and Hydraulic Conductivity of Compacted Clay. *Eng. Geol.* **2020**, *267*, 105505. [CrossRef]
29. Akcanca, F.; Aytekin, M. Impact of Wetting-Drying Cycles on the Hydraulic Conductivity of Liners Made of Lime-Stabilized Sand-Bentonite Mixtures for Sanitary Landfills. *Environ. Earth Sci.* **2014**, *72*, 59–66. [CrossRef]
30. Benchouk, A.; Derfouf, F.M.; Nabil, A. Behavior of Some Clays on Drying and Wetting Paths. *Arab. J. Geosci.* **2013**, *6*, 4565–4573. [CrossRef]
31. Umezakin, T.; Kawamura, T. Shrinkage and Desaturation Properties during Desiccation of Reconstituted Cohesive Soil. *Soils Found.* **2013**, *53*, 47–63. [CrossRef]
32. Mishra, A.K.; Dhawan, S.; Rao, S.M. Analysis of Swelling and Shrinkage Behavior of Compacted Clays. *Geotech. Geol. Eng.* **2008**, *26*, 289–298. [CrossRef]
33. Ma, T.; Wei, C.; Yao, C.; Yi, P. Microstructural Evolution of Expansive Clay during Drying–Wetting Cycle. *Acta Geotech.* **2020**, *15*, 2355–2366. [CrossRef]
34. Wu, Y.; Li, L.; Feng, X.; Zhang, R.; Ákos, T. Effect of Cyclic Wetting and Drying on the Microstructure of Slip Zone Soils in Huangtupo Landslide. *J. Eng. Sci. Technol. Rev.* **2016**, *9*, 209–216. [CrossRef]
35. Estabragh, A.R.; Moghadas, M.; Javadi, A.A. Hydrochemical Effect of Different Quality Of Water on The Behaviour of an Expansive Soil During Wetting and Drying Cycles. *Irrig. Drain.* **2016**, *65*, 371–381. [CrossRef]
36. Rao, K.S.S.; Rao, S.M.; Gangadhara, S. Swelling Behaviour of a Desiccated Clay. *Geotest. J.* **2000**, *23*, 193–198. [CrossRef]
37. Nowamooz, H.; Masrouri, F. Hydromechanical Behaviour of an Expansive Bentonite/Silt Mixture in Cyclic Suction-Controlled Drying and Wetting Tests. *Eng. Geol.* **2008**, *101*, 154–164. [CrossRef]
38. Zhang, R.; Yang, H.; Zheng, J. *The Effect of Vertical Pressure on the Deformation and Strength of Expansive Soil during Cyclic Wetting and Drying*; Geotechnical Special Publications (GSP): Reston, VA, USA, 2006; pp. 894–905. [CrossRef]
39. Basma, A.A.; Al-Homoud, A.S.; Al-Tabari, E.Y. Effects of Methods of Drying on the Engineering Behavior of Clays. *Appl. Clay Sci.* **1994**, *9*, 151–164. [CrossRef]
40. Tawfiq, S.; Nalbantoglu, Z. Swell-Shrink Behavior of Expansive Clays. In Proceedings of the 2nd International Conference on New Developments in Soil Mechanics and Geotechnical Engineering, Near East University, Nicosia, North Cyprus, 28–30 May 2009; pp. 28–30.
41. Subba Rao, K.S.; Satyadas, G.C. Swelling Potential with Cycles of Swelling and Partial Shrinkage. In Proceedings of the 6th International Conference on Expansive, New Delhi, India, 1–4 December 1987; pp. 137–142.
42. Chen, F.H. The Use of Piers to Prevent the Uplifting of Lightly Loaded Structures Founded on Expansive Soils. In Proceedings of the International Research and Engineering Conference on Expansive Clay Soils, College Station, TX, USA, 30 August–3 September 1965.
43. Chen, F.H.; Ma, G.S. Swelling and Shrinkage Behaviour of Expansive Clays. In Proceedings of the 6th International Conference on Expansive, New Delhi, India, 1–4 December 1987; pp. 127–129.
44. Popescu, M.E. Behaviour of Expansive Soils with Crumb Structures. In Proceedings of the Fourth International Conference on Expansive Soils, Denver, CO, USA, 16–18 June 1980; pp. 158–171.
45. Osipov, V.I.; Bik, N.N.; Rumjantseva, N.A. Cyclic Swelling of Clays. *Appl. Clay Sci.* **1987**, *2*, 363–374. [CrossRef]
46. Nowamooz, H. Equilibrium Stage of Soil Cracking and Subsidence after Several Wetting and Drying Cycles. *Geotechnics* **2023**, *3*, 193–211. [CrossRef]

47. Abbas, M.F.; Shaker, A.A.; Al-Shamrani, M.A. Hydraulic and Volume Change Behaviors of Compacted Highly Expansive Soil under Cyclic Wetting and Drying. *J. Rock Mech. Geotech. Eng.* **2023**, *15*, 486–499. [CrossRef]
48. Nowamooz, H.; Masrouri, F. Shrinkage/Swelling of Compacted Clayey Loose and Dense Soils. *C. R. Mec.* **2009**, *337*, 781–790. [CrossRef]
49. Dif, A.E.; Bluemel, W.F. Expansive Soils under Cyclic Drying and Wetting. *Geotech. Test. J.* **1991**, *14*, 96–102. [CrossRef]
50. Dafalla, M.; Shaker, A.A.; Al-Shamrani, M. Influence of Wetting and Drying on Swelling Parameters and Structure Performance. *J. Perform. Constr. Facil.* **2019**, *33*, 04018101. [CrossRef]
51. Sharma, R.S.; Wheeler, S.J. Behaviour of an Unsaturated Highly Expansive Clay during Cycles of Wetting and Drying. In Proceedings of the Unsaturated Soils for Asia, Singapore, 18–19 May 2000; pp. 721–726.
52. Huang, S.; Barbour, S.L.; Fredlund, D.G. Development and Verification of a Coefficient of Permeability Function for a Deformable Unsaturated Soil. *Can. Geotech. J.* **1998**, *35*, 411–425. [CrossRef]
53. Romero, E.; Gens, A.; Lloret, A. Water Permeability, Water Retention and Microstructure of Unsaturated Compacted Boom Clay. *Eng. Geol.* **1999**, *54*, 117–127. [CrossRef]
54. Watabe, Y.; Leroueil, S.; Le Bihan, J.P. Influence of Compaction Conditions on Pore-Size Distribution and Saturated Hydraulic Conductivity of a Glacial Till. *Can. Geotech. J.* **2000**, *37*, 1184–1194. [CrossRef]
55. Deng, Y.F.; Tang, A.M.; Cui, Y.J.; Li, X.L. Study on the Hydraulic Conductivity of Boom Clay. *Can. Geotech. J.* **2011**, *48*, 1461–1470. [CrossRef]
56. Sridharan, A.; Nagaraj, H.B. Hydraulic Conductivity of Remolded Fine-Grained Soils versus Index Properties. *Geotech. Geol. Eng.* **2005**, *23*, 43–60. [CrossRef]
57. Leroueil, S.; Le Bihan, J.P.; Sebaihi, S.; Alicescu, V. Hydraulic Conductivity of Compacted Tills from Northern Quebec. *Can. Geotech. J.* **2002**, *39*, 1039–1049. [CrossRef]
58. Abbas, M.F.; Elkady, T.Y.; Aldrees, A.A.; Shaker, A.A. Impact of Stress Path on Hydraulic and Mechanical Behavior of Compacted Al-Qatif Clay. *Transp. Geotech.* **2021**, *26*, 100417. [CrossRef]
59. Huang, S.; Fredlund, D.G.; Barbour, S.L. Measurement of the Coefficient of Permeability for a Deformable Unsaturated Soil Using a Triaxial Permeameter. *Can. Geotech. J.* **1998**, *35*, 426–432. [CrossRef]
60. Shear, D.; Olsen, H.; Nelson, K. *Effects of Desiccation on the Hydraulic Conductivity Versus Void Ratio Relationship for a Natural Clay*; Transportation Research Board: Washington, DC, USA, 1992; pp. 130–135. Available online: https://trid.trb.org/view/371568 (accessed on 18 April 2023).
61. Louati, F.; Trabelsi, H.; Jamei, M. Exprimental and Numerical Investigation about Permeability of Clay Subjected to Humidification-Desiccation Cycles. In Proceedings of the 3ème Colloque International sur les sols non Satures (UNSAT Batna 2015), Batna, Algeria, 16–17 November 2015.
62. Albrecht, B.A.; Benson, C.H. Effect of Desiccation on Compacted Natural Clays. *J. Geotech. Geoenviron. Eng.* **2001**, *127*, 67–75. [CrossRef]
63. Day, R.W. Discussion of Hydraulic Conductivity of Desiccated Geosynthetic Clay Liners. *J. Geotech. Geoenviron. Eng. ASCE* **1997**, *123*, 484–486. [CrossRef]
64. Louati, F.; Trabelsi, H.; Mehrez, J.; Taibi, S. Wet- Dry Cycles Effect on the Saturated Hydraulic Conductivity. In Proceedings of the 7th International Conference on Unsaturated Soils, UNSAT2018, Hongkong, China, 3–5 August 2018.
65. Day, R.W. Discussion: Infiltration Tests on Fractured Compacted Clay. *J. Geotech. Geoenviron. Eng.* **1998**, *124*, 1149–1152. [CrossRef]
66. Azam, S. Influence of Mineralogy on Swelling and Consolidation of Soils in Eastern Saudi Arabia. *Can. Geotech. J.* **2003**, *40*, 964–975. [CrossRef]
67. Al-Sayari, S.J.; Zotl, J.G. *Quaternary period in Saudi Arabia*; Springer: Vienna, Austria, 1978.
68. El-Naggar, Z. Foundation problems in sabkha deposits. In *Short Course on Foundation Engineering for Practicing Engineers*; CE Department, KFUPM: Dhahran, Saudi Arabia, 1988; pp. SD1–SD54.
69. Azam, S.; Abduljauwad, S.N.; Al-Shayea, N.A.; Al-Amoudi, O.S.B. Expansive Characteristics of Gypsiferous/Anhydritic Soil Formations. *Eng. Geol.* **1998**, *51*, 89–107. [CrossRef]
70. Al-Shayea, N.A. The Combined Effect of Clay and Moisture Content on the Behavior of Remolded Unsaturated Soils. *Eng. Geol.* **2001**, *62*, 319–342. [CrossRef]
71. Elkady, T.Y.; Shaker, A.A.; Dhowain, A.W. Shear Strengths and Volume Changes of Sand–Attapulgite Clay Mixtures. *Bull. Eng. Geol. Environ.* **2015**, *74*, 595–609. [CrossRef]
72. Shaker, A.A.; Elkady, T.Y. Hydraulic Performance of Sand–Clay Mixtures: Soil Fabric Perspective. *Géotechn. Lett.* **2015**, *5*, 198–204. [CrossRef]
73. Shaker, A.A.; Elkady, T.Y. Investigation of the Hydraulic Efficiency of Sand-Natural Expansive Clay Mixtures. *Int. J. GEOMATE* **2016**, *10*, 1790–1795.
74. Abbas, M.F. Multi-Dimensional Hydro-Mechanical Behavior of Compacted Highly Expansive Soils. Ph.D. Thesis, King Saud University, Riyadh, Saudi Arabia, 2016.
75. *ASTM D698*; Standard Test Methods for Laboratory Compaction Characteristics of Soil Using Standard Effort (12,400 Ft-Lbf/Ft3 (600 KN-m/M3)). ASTM International: West Conshohocken, PA, USA, 2000.
76. *ASTM D4546*; Standard Test Methods for One-Dimensional Swell or Settlement Potential of Cohesive. ASTM International: West Conshohocken, PA, USA, 2003.

77. Gens, A.; Alonso, E.E. A Framework for the Behaviour of Unsaturated Expansive Clays. *Can. Geotech. J.* **1992**, *29*, 1013–1032. [CrossRef]
78. Alonso, E.E.; Vaunat, J.; Gens, A. Modelling the Mechanical Behaviour of Expansive Clays. *Eng. Geol.* **1999**, *54*, 173–183. [CrossRef]